Current Optics and Photonics
Vol. 4, No. 6, December 2020, pp. 516-523

ISSN: 2508-7266(Print) / ISSN: 2508-7274(Online)
DOI: https://doi.org/10.3807/COPP.2020.4.6.516

Photorealistic Ray-traced Visualization of Manufacturing Tolerances of Freeform Vehicle Side Mirror

Syed Azkar Ul Hasan[1], Hocheol Lee[1]*, Gang Lee[2], and Sungkoo Lee[2]

[1]*Department of Mechanical Engineering, Hanbat National University, Daejeon 34158, Korea*
[2]*R&D Institute Bullsone Co. Ltd., Incheon 21984, Korea*

(Received July 27, 2020 : revised September 18, 2020 : accepted October 18, 2020)

The normal low-cost manufacturing process for freeform vehicle side mirrors causes deviations from the design curvature. Here, an improved manufacturing process is proposed, combining photorealistic ray-traced visualization of each deviation and subsequent analysis of its deviated reflective scene compared to that of the original design. The proposed mechanism successfully highlights the overlap and mismatch regions of deviated reflected scenes with reference to the desired reflective scenes. We benchmarked the robustness of freeform mirror manufacturing by evaluating the 10, 20, and 30% root-mean-square (RMS) deviated curvature, and concluded that the acceptable deviation needs to be below RMS20% to avoid mismatched regions that could mislead the driver.

Keywords : Photorealistic ray-traced visualization, Free-form vehicle side-mirror, Manufacturing tolerances, Slumping process
OCIS codes : (080.2208) Fabrication, tolerancing; (220.4610) Optical fabrication; (230.4040) Mirrors; (240.6700) Surfaces

I. INTRODUCTION

A safe and comfortable driving environment plays a crucial role in improving the level of silent communication among drivers [1]. Smooth communication while driving mainly depends on the visibility of the rear-view environment through the rear-view mirrors, and it implicitly affects the behavior of the driver to a considerable extent [2]. Visual blind spots pose a certain level of risk while changing lanes or otherwise maneuvering [3-5]. Using freeform vehicle side mirrors having multi-radius curvature enhances the visibility of the rear-view environment and improves safety while executing lane changes [6]. Moreover, a freeform side mirror provides a wider field of view as opposed to flat and spherical vehicle mirrors, thereby reducing or eliminating the potential danger of a blind spot [7].

Enhancement of visibility in case of freeform mirrors involves slight minification of image features pertaining to the rear-view environment [8]. This minification of image in the case of nonplanar mirrors has brought into question their use for the driver side of the vehicle in some safety regulations, arguing that it can be misleading for judging the actual distance of the following vehicle. In the U.S. regulations, the use of a nonplanar mirror is restricted to the passenger side of the vehicle only, whereas European and Korean regulations allow nonplanar mirrors on both the sides of the vehicle [9, 10]. As per Korean regulations, the radius of curvature of a nonplanar mirror needs to be greater than 1200 mm as a tradeoff between a larger field of view and slight image minification.

The manufacturing of freeform mirrors can be accomplished through polishing, hot slumping process, injection molding, and hot embossing [11]. However, a low-cost, high-volume slumping process is the optimal choice for manufacturing for fabrication of freeform mirrors [12-14]. The heating rate and soaking temperature [15] during the slumping process play a vital role in the formation of the desired curvature. In addition, an open-ended environment

*Corresponding author: hclee@hanbat.ac.kr, ORCID 0000-0001-7436-7567
Color versions of one or more of the figures in this paper are available online.

along with a moving conveyer during the mass production slumping process obviates strict temperature control [16, 17] and results in certain manufacturing deviations from the designed curvature profile. The deviated curvature for the freeform mirror can have a variety of scenarios that can be either allowable/tolerable or detrimental compared to the design goal of providing true representation of the rear-view environment through the side mirror of the vehicle.

Photorealistic ray-traced visualization provides a platform for acquiring virtual images of geometrically variant optical surfaces [18, 19]. Three-dimensional reconstruction of motor vehicles by using the structured light scans of a virtual mirror surface and tracking the associated visibility lines were effectively used to identify the potential root cause of traffic violations [20]. In the real scenarios, deviation from the ideal design affect the reconstruction of large-area optical surfaces through curvature data measurement. [21, 22]. Realization of progressive-addition lens design became possible by combining the reconstruction and optimization [23, 24].

Photorealistic realization is capable of obviating or reducing the experimental requirement similar to visualization of invisibility cloaks [25]. Additionally, our previous work [26] demonstrated the potential of photorealistic ray-traced visualization for acquiring the virtual reflective scenes for enhancing the visibility in freeform vehicle mirrors.

To evaluate whether the manufacturing deviation during the slumping process is consistent, here we suggest a combined framework of photorealistic ray-traced visualization and subsequent analysis of the reflective scene with reference to the designed reflective scene, as illustrated schematically in Fig. 1. In the following text we will highlight the potentials of this simple and novel approach to rule out the unacceptable deviations, thereby improving the manufacturing tolerance design through back-and-forth interaction between the design, manufacturing, and simulation followed by analysis. The schematic of photorealistic ray-traced visualization for the reference images has been illustrated in Fig. 2.

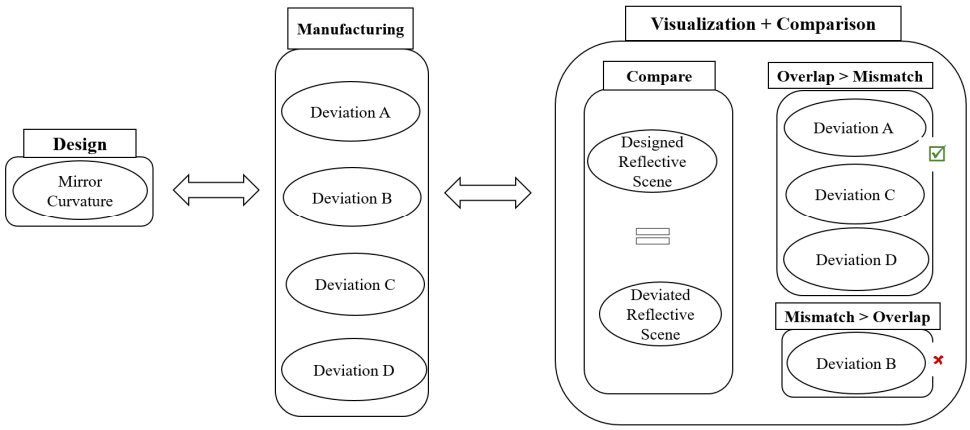

FIG. 1. Schematic diagram of the improved design mechanism for a freeform vehicle mirror using a combined framework of photorealistic ray-traced visualization, and Adobe Photoshop reflective scene analysis.

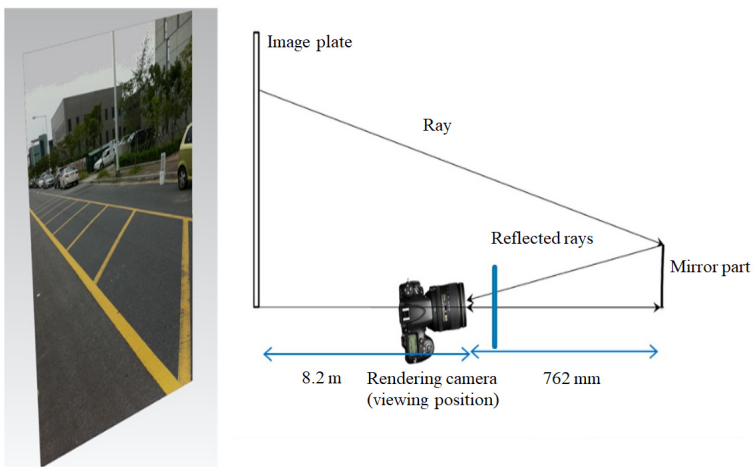

FIG. 2. Schematic diagram of photorealistic ray-traced visualization for the reference image (left) used for manufacturing deviation-incorporated reflective scenes. Reprinted with permission from [26] © The Optical Society of America.

II. GENERATION OF FREEFORM MANUFACTURING TOLERANCES AND ASSOCIATED PHOTOREALISTIC RAY-TRACED VISUALIZATION

The measurement of post-slumping-process curvature was carried out using a coordinate measuring machine, which revealed that four typical types of deviations are involved during the slumping process of a horizontal progressive side mirror. For the sake of convenience, we will refer to these deviation curvatures as A, B, C, D in the following paragraphs. The characteristic curve associated with the design and each above-mentioned deviation is shown in Figs. 3(a)-3(e).

Photorealistic ray-traced visualization for the design curvature as well as deviations A, B, C, D and RMS10%

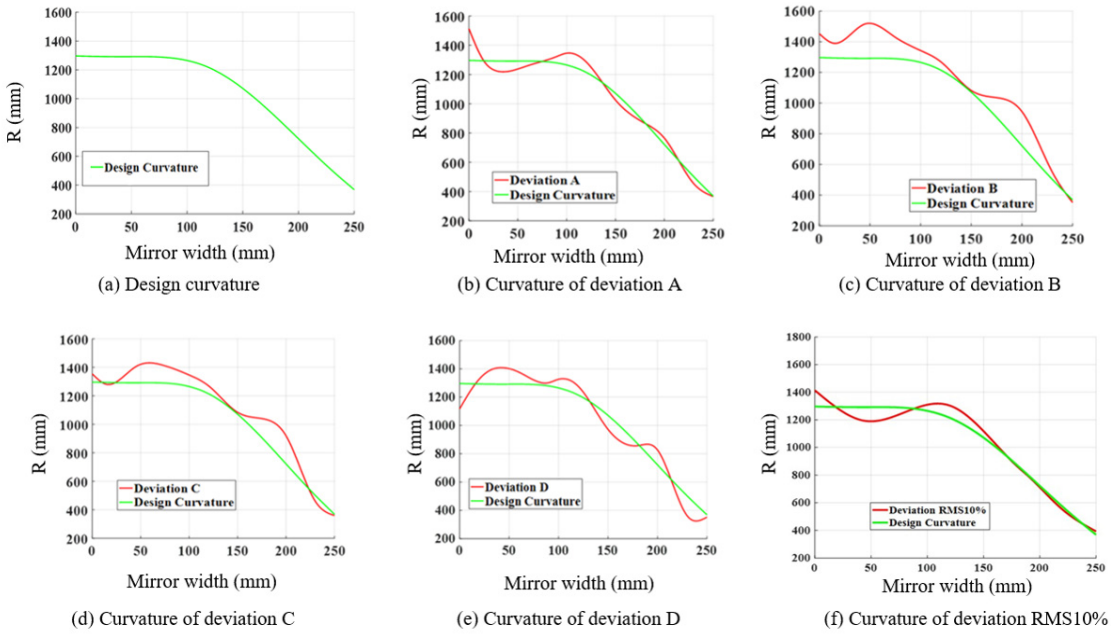

(a) Design curvature (b) Curvature of deviation A (c) Curvature of deviation B

(d) Curvature of deviation C (e) Curvature of deviation D (f) Curvature of deviation RMS10%

FIG. 3. Comparison of design and deviated curvature: (a) design curvature (b)-(e) deviation A, B, C, D, and (f) RMS10%.

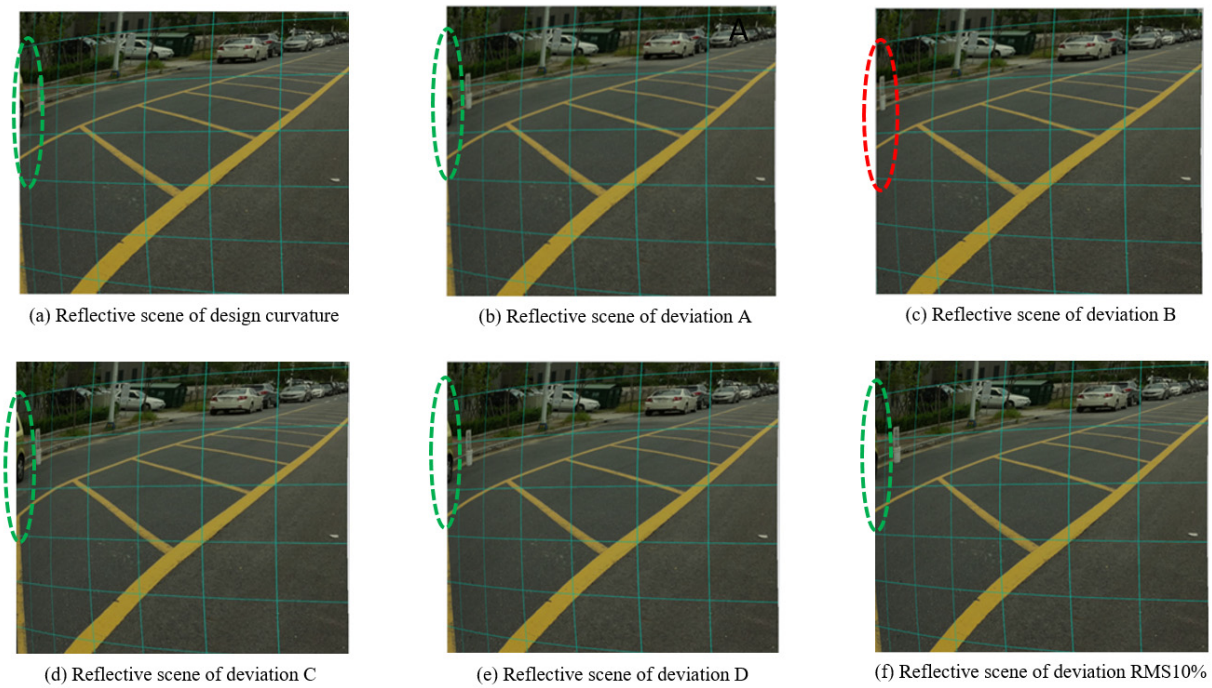

(a) Reflective scene of design curvature (b) Reflective scene of deviation A (c) Reflective scene of deviation B

(d) Reflective scene of deviation C (e) Reflective scene of deviation D (f) Reflective scene of deviation RMS10%

FIG. 4. Reflective scenes for (a) design curvature (b-f) A, B, C, D, RMS10% manufacturing deviations.

is shown in Figs. 4(a)-4(f). A closer look of the reflective scenes in the green and red dotted oval lines in Fig. 4 reveal that the rear end of the light green car is absent in the reflective scene associated with deviation B (Fig. 4(c)) and the enhanced visibility pertains to deviations C and D (Figs. 4(d), 4(e)), which highlight the potential of photo-realistic visualization to capture the rear-view environment surrounding the vehicle based on the developed curvature of a driver-side rear-view mirror. Similarly, we hypothetically generated root-mean-square (RMS) 10, 20, 30% deviated curvature (for deviation A) to evaluate the robustness of the slumping process. Figures 4(f), 5(a), 5(b) illustrate the photorealistic ray-traced visualization associated with the freeform curvature for the RMS10, 20, and 30% deviations. This can lead to the incorporation of a blind spot as shown in Fig. 4(c). The overall effect for deviations A, C, and D is not contradictory with respect to our design goal, because the mismatch region is considerably smaller compared to the overlap area pertaining to these deviations.

III. REFLECTIVE SCENE ANALYSIS OF FREEFORM MIRROR MANUFACTURING DEVIATIONS

To understand whether the rear-view environment representation is useful for the driver, the effectiveness of each deviated curvature reflective scene was compared to that of the design curvature reflective scene (Fig. 4(a)) using Adobe Photoshop. The yellow parking lines in the design curvature reflective scene, visible in the driver's side mirror, were converted to blue, whereas the yellow parking lines

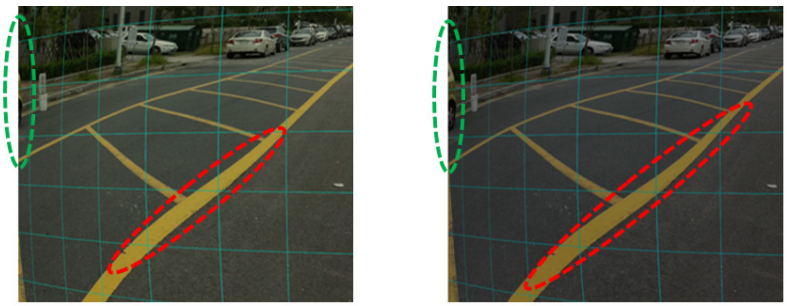

(a) Reflective scene of deviation RMS20% (b) Reflective scene of deviation RMS30%

FIG. 5. Reflective scenes for (a) RMS20%, (b) RMS30% manufacturing deviations.

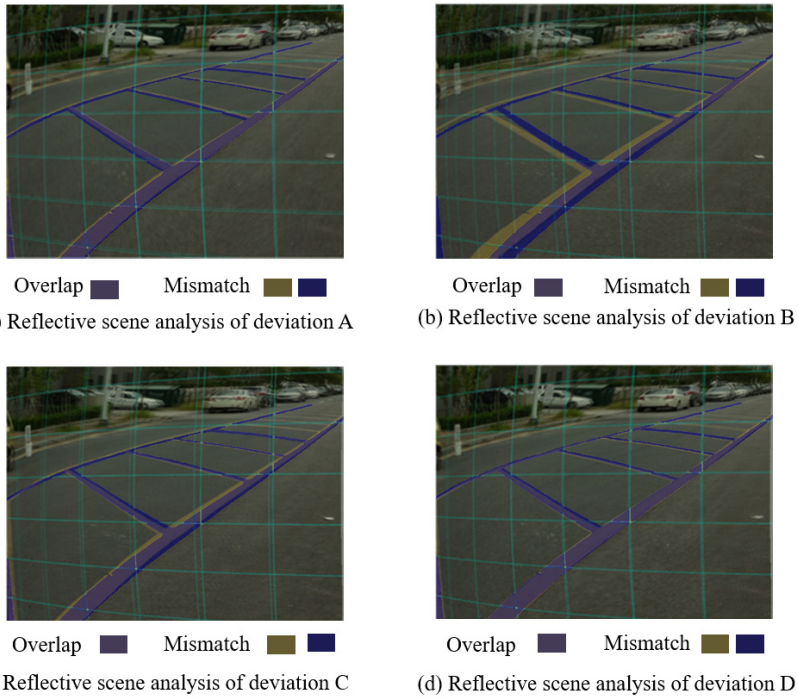

(a) Reflective scene analysis of deviation A (b) Reflective scene analysis of deviation B

(c) Reflective scene analysis of deviation C (d) Reflective scene analysis of deviation D

FIG. 6. Analysis of reflective scenes for the deviations (a-d) A, B, C, D by superimposing the deviated reflected scene over the design curvature reflected scene to highlight the overlap and mismatch associated with each deviation.

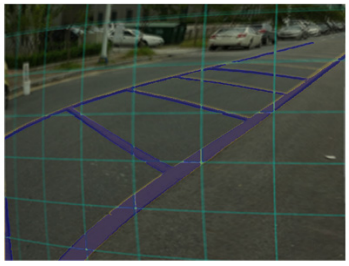

(a) Reflective scene analysis of deviation RMS10%

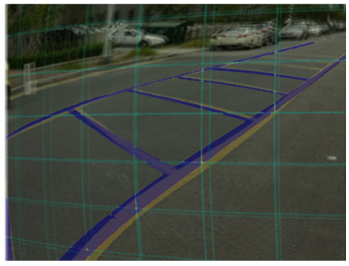

(b) Reflective scene analysis of deviation RMS20%

FIG. 7. Analysis of reflective scenes for the deviations (a) RMS10% and (b) RMS20% by superimposing the deviated reflected scene over the design curvature reflected scene to highlight the overlap and mismatch associated with each deviation.

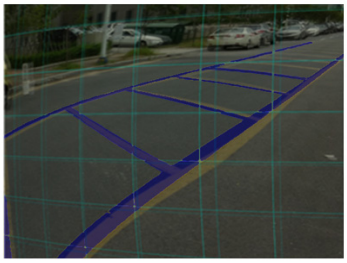

FIG. 8. Analysis of reflective scenes for the deviations RMS30% by superimposing the deviated reflected scene over the design curvature reflected scene to highlight the overlap and mismatch associated with each deviation.

represent the deviated reflective scene for all the deviations A, B, C, and D. Afterwards, each deviated reflective scene was superimposed over the design curvature reflective scene to highlight the mismatch and overlap regions between the deviated curvature reflective scene and the design curvature reflective scene. The yellow and blue color followed by superimposing reflective scenes points towards the mismatch between deviated and design curvature in terms of associated reflective scenes respectively. This simple approach clearly demonstrated the advantages and disadvantages associated with a typical deviation and has the potential to be used effectively during the manufacturing process design. The mismatch and overlap areas pertaining to the deviation A, B, C, D are shown in Fig. 6.

In particular, the usefulness of a typical deviation can be easily determined based on the extent of its overlap with the design curvature reflective scene. As illustrated in Fig. 6(b), deviation B yellow parking lines have a small overlap as compared to the design curvature blue parking lines; therefore, this deviation is not desirable and must be ruled out during the design and manufacturing process to avoid any potential danger of incorrect representation of rear-view environment for the driver. Additionally, the large mismatch associated with the deviation B reflective scene over the design curvature reflected scene to highlight the overlap and mismatch regions associated with each deviation.

Similarly, we compared the RMS10% deviation and the RMS20% deviation (deviation A type) with the designed curvature, and the corresponding overlap and mismatch regions have been highlighted in Fig. 7, whereas the overlap and mismatch pertaining to RMS30% deviation has been highlighted in Fig. 8.

IV. HORIZONTAL IMAGE SHRINKAGE OF FREEFORM MIRROR

Freeform manufacturing deviation might affect the regions associated with the rear-view environment; therefore, we compared the horizontal shrinkage of image features for the design as well as the deviation curvature. As the difference in curvature along the lateral (vertical) direction of mirror is negligible, the horizontal image shrinkage analysis is performed at the center line of the mirror ($y = 100$ mm) using the measurement module of Adobe Photoshop. The reference image is composed of black rectangles separated by white lines, as illustrated in Fig. 9(a). Figure 9(b) illustrates the photorealistic ray-traced visualization for the design curvature of freeform vehicle mirror. The length of segment between two consecutive points in Fig. 9 corresponds to the broadening or shrinking of horizontal length of black rectangles along the horizontal axis of the mirror, thereby highlighting expansion and contraction of image features associated with any deviated curvature.

Figure 10 illustrates the relative broadening and contraction of black rectangles and white lines for deviations A, B, C, and D, which imply the combination of shrinkage and expansion zones for the realization of reflective scene for the respective curvatures. The insight derived from the expansion and contraction zones for their features in the reflective scene highlights the sensitive areas associated with typical curvature deviations, thereby contributing to an improvement in the design, as depicted in Figs. 11 and 12.

Moreover, the magnitude of image shrinkage along the horizontal mirror axis reveals the extent of image shrinkage

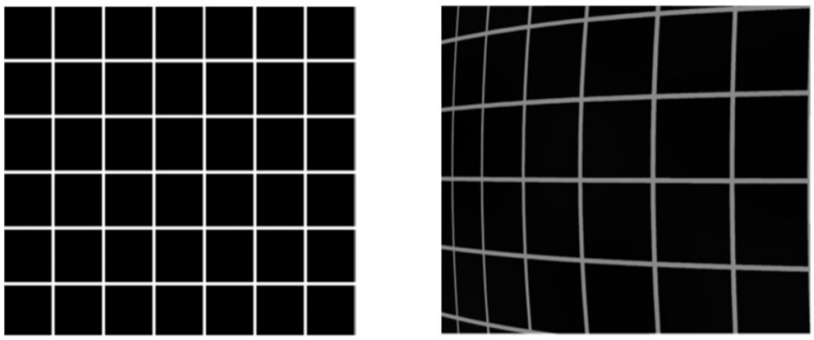

(a) Reference grid (b) Freeform design curvature

FIG. 9. Photorealistic visualization of (a) reference grid and (b) freeform design curvature to obtain insight on the shrinkage and elongation of image features along the longitudinal axis of the freeform mirror.

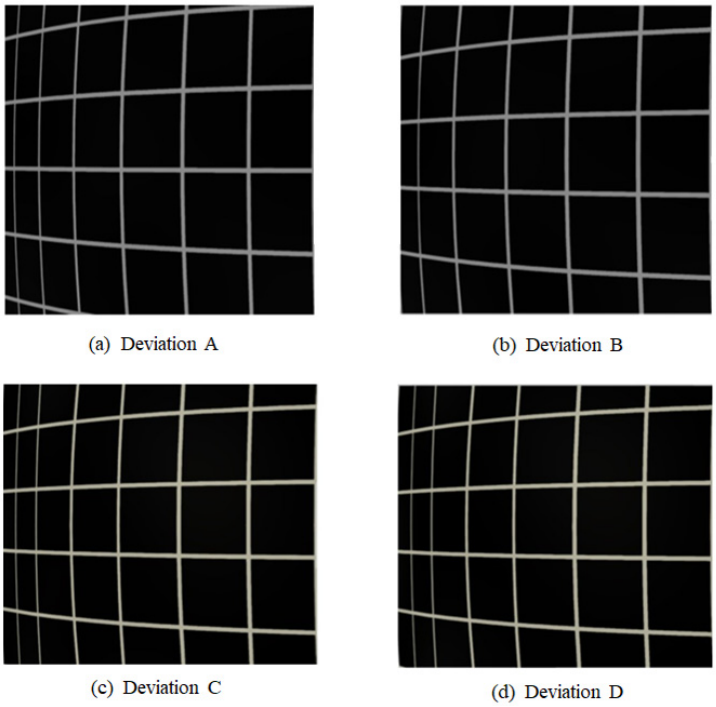

(a) Deviation A (b) Deviation B

(c) Deviation C (d) Deviation D

FIG. 10. Photorealistic visualization of (a) deviation A, (b) deviation B, (c) deviation C, and (d) deviation D for horizontal image shrinkage analysis in Adobe Photoshop.

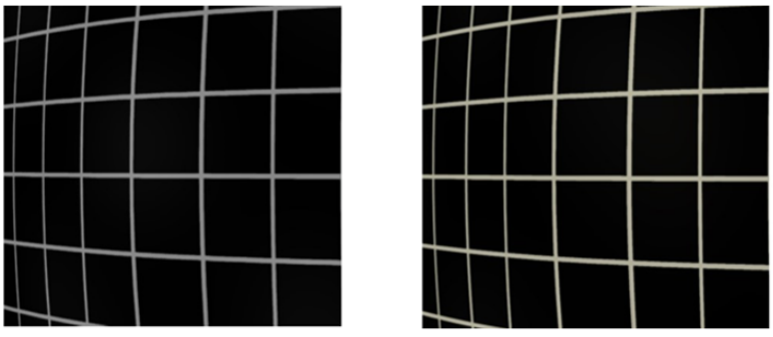

(a) Deviation RMS 10% (b) Deviation RMS 20%

FIG. 11. Photorealistic visualization of (a) RMS10% deviation for deviation A and (b) RMS20% deviation of deviation A for horizontal image shrinkage analysis in Adobe Photoshop.

for the features of rear-view environment visible in the driver's side rear-view mirror. This simple approach enables us to design and optimize the manufacturing process for excluding the undesired excessive shrinkage of features, in order to avoid the misrepresentation of the rear-view environment.

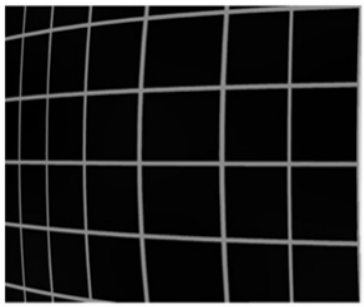

FIG. 12. Photorealistic visualization of RMS30% deviation of deviation A for horizontal image shrinkage analysis in Adobe Photoshop.

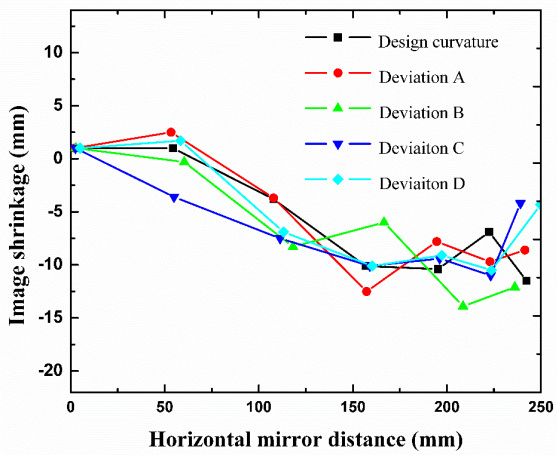

FIG. 13. Horizontal image shrinkage along the mirror distance for the design and deviated curvature reflective scenes.

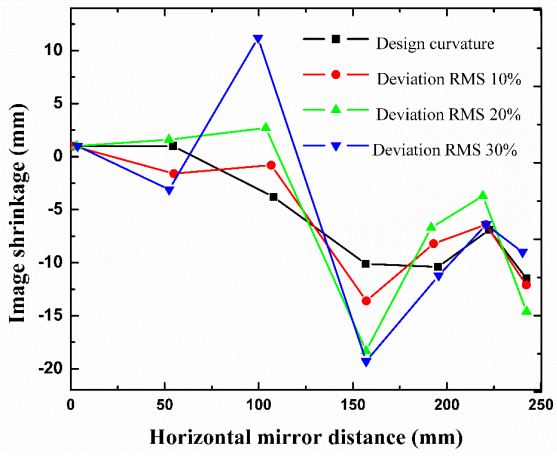

FIG. 14. Horizontal image shrinkage along the mirror distance for the design and RMS deviated curvature reflective scenes.

A careful review of Fig. 13 reveals that the maximum image shrinkage is -13.9 mm in the case of deviation B, whereas deviation D represents maximum field of view for the driver by combining its constituent shrinkage and expansion zones along the horizontal mirror axis. The images's shrinkage for the RMS (10, 20, 30%) deviations were compared with that of the design curvature as shown in Fig. 14 to evaluate the robustness of the low-cost high-end slumping process.

RMS30% deviation clearly depicts the abrupt excessive expansion and shrinkage of the horizontal progressive driver's side mirror. Similarly, the expansion and contraction zones associated with the RMS10% and RMS20% deviations are illustrated in Fig. 11, whereas that for the RMS30% deviation clearly depicts an abrupt excessive expansion and shrinkage of image between the 100-150 mm horizontal region of the mirror, and the associated reflective scene cannot be a true representation of the rear-view environment for the driver. This approach can be used effectively to design the tolerance system for the manufacturing process, in order to remove the undesired deviation during the manufacturing of the driver's side mirror.

V. CONCLUSION

We successfully introduced a simple and novel approach to gain insight on the virtues and limitations associated with any deviation and its consequences in the form of reflective scenes available at the side mirrors of vehicles. The acceptable deviations can be incorporated into the manufacturing process through design optimization, whereas the detrimental deviations can be removed by improving the manufacturing design for freeform mirrors. Benchmarking of the robust freeform manufacturing process design of vehicle mirrors was accomplished in order to avoid any misleading interpretation the driver may receive, and this approach can be further extended towards the development of a complete tolerance system. In addition, the expansion and shrinkage zone analysis associated with manufacturing process deviation along the horizontal direction of a free-form mirror provides useful information for the features in the rear-view environment. Moreover, it was revealed that tolerable deviations below RMS20% involve less mismatch and greater overlap regions, similar to the freeform design curvature surface.

ACKNOWLEDGMENT

This study was financially supported by Hanbat National University Financial Accounting Research Fund, 2018 year.

REFERENCES

1. C. F. Wu, C. J. Lin, H. Y. Lin, and H. Chung, "Adjacent lane detection and lateral vehicle distance measurement using vision-based neuro-fuzzy approaches," J. Appl. Res. Technol. **11**, 251-258 (2013).
2. T. Zimasa, S. Jamson, and B. Henson, "Are happy drivers safer drivers? Evidence from hazard response time and eye tracking data," Transp. Res. Part F. Traffic Psychol. Behav. **46**, 14-23 (2017).
3. K. L. Young and P. M. Salmon, "Examining the relationship between driver distraction and driving errors: A discussion of theory, studies and methods," Saf. Sci. **50**. 165-174 (2012).
4. J. Kuwana, M. Itoh, and T. Inagaki, "Dynamic side-view mirror: assisting situation awareness in blind spots," in *Proc. IEEE Intelligent Vehicles Symposium - IV* (Gold Coast, QLD, Australia, Jun. 2013), pp. 455-460.
5. Y. Gao, C. Lin, Y. Zhao, X. Wang, S. Wei, and Q. Huang, "3-D surround view for advanced driver assistance system," IEEE Trans. Intell. Transp. Syst. **19**, 320-328 (2018).
6. T. Ehlgen, T. Pajdla, and D. Ammon, "Eliminating blind spots for assisted driving," IEEE Trans. Intell. Transp. Syst. **9**, 657-665 (2008).
7. H. Lee, D. Kim, and S. Yi, "Horizontally progressive mirror for blind spot detection in automobiles," Opt. Lett. **38**, 317-319 (2013).
8. D. Moukhwas, "Road junction convex mirrors," Appl. Ergon. **18**, 133-136 (1987).
9. J. Schumann, M. Sivak, and M. J. Flannagan, "Are driver-side convex mirror helpful or harmful?," Int. J. Vehicle Des. **19**, 29-40 (1998).
10. J. Luoma, M. J. Flannagan, and M. Sivak, "Effect of non-planar driver-side mirrors on lane-change crashes," Transp. Hum. Factors **2**, 279-289 (2000).
11. F. Z. Fang, X. D. Zhang, A. Weckenmann, G. X. Zhang, and C. Evans, "Manufacturing and measurement of freeform optics," CIRP Ann. Manuf. Technol. **62**, 823-846 (2013).
12. Y. Chen and A. Y. Yi, "Design and fabrication of freeform glass concentrating mirrors using a high volume thermal slumping process," Sol. Energy Materkj Sol. Cells **95**, 1654-1664 (2011).
13. M. B. Boubaker, B. L. Corre, Y. Meshaka, and G. Jeandel, "Finite element simulation of the slumping process of a glass plate using 3D generalized viscoelastic Maxwell model," J. Non Cryst. Solids **405**, 45-54 (2014).
14. T. Stalcup, K. Hammer, D. Lesser, B. Olbert, S. Warner, B. Wheelwright, R. Angel, and J. Villaneuva, "Initial results of advanced glass slumping for commercial CSP systems," in *Renewable Energy and Environment* (Optical Society of America, 2013), paper RT2D.6.
15. D. Zhao, P. Liu, L. He, and B. Chen, "Numerical and experimental investigation of heating process of glass thermal slumping," J. Opt. Soc. Korea **20**, 314-320 (2016).
16. B. Salmaso, M. Civitani, C. Brizzolari, S. Basso, M. Ghigo, G. Pareschi, D. Spiga, L. Proserpio, and Y. Suppiger, "Development of mirrors made of chemically tempered glass foils for future X-ray telescopes," Exp. Astron. **39**, 527-545 (2015).
17. H. Lee, G. Lee, S. Lee, and J. Kim, "Slumping process of the horizontally progressive type of automobile side mirror," in *Classical Optics* (Optical Society of America, 2014), paper OW2B.2.
18. R. A. Hicks, "Controlling a ray bundle with free-form reflector," Opt. Lett. **33**, 1672-1674 (2008).
19. G. Dolling, M. Wegener, S. Linden, and C. Hormann, "Photorealistic image of objects in effective negative-index materials," Opt. Express, **14**, 1842-1849 (2006).
20. A. Leipner, E. Dobler, M. Braun, T. Sieberth, and L. Ebert, "Simulation of mirror surfaces for virtual estimation of visibility lines for 3D motor vehicle collision reconstruction," Forensic Sci. Int. **279**, 106-111 (2017).
21. C. Elster, J. Gerhardt, P. Thomsen-Schmidt, M. Schulz, and I. Weingartner, "Reconstructing surface profiles from curvature measurements," Optik, **113**, 154-158 (2002).
22. D. W. Kim, B. C. Kim, C. Zhao, C. Oh, and J. H. Burge, "Algorithm for surface reconstruction from curvature data for freeform aspherics," Proc. SPIE **8838**, 88380B (2013).
23. W. Jiang, W. Bao, Q. Tang, and H. Wang, "A variational-difference numerical method for designing progressive-addition lenses," Comput. Aided Des. **48**, 17-27 (2014).
24. L. Qin, L. Qian, and J. Yu, "Simulation method for evaluating progressive addition lenses," Appl. Opt. **52**, 4273-4278 (2013).
25. J. C. Halimeh and M. Wegener, "Photorealistic rendering of unidirectional free space invisibility cloaks," Opt. Express **21**, 9457-9472 (2013).
26. H. Lee, K. Kim, G. Lee, S. Lee, and J. Kim, "Photorealistic ray tracing to visualize automobile side mirror reflective scenes," Opt. Express **22**, 25729-25738 (2014).